Hindawi Publishing Corporation
Journal of Nanomaterials
Volume 2013, Article ID 517643, 6 pages
http://dx.doi.org/10.1155/2013/517643

Research Article

Characterization of Newly Synthesized $ZrFe_2O_5$ Nanomaterial and Investigations of Its Tremendous Photocatalytic Properties under Visible Light Irradiation

Shaukat Ali Shahid,[1] Ayman Nafady,[2] Inam Ullah,[3] Yun H. Taufiq-Yap,[4] Imran Shakir,[5] Farooq Anwar,[6] and Umer Rashid[7]

[1] *Department of Physics, University of Agriculture, Faisalabad 38040, Pakistan*
[2] *Department of Chemistry, College of Science, King Saud University, Riyadh 11451, Saudi Arabia*
[3] *Department of Chemistry & Biochemistry, University of Agriculture, Faisalabad 38040, Pakistan*
[4] *Catalysis Science and Technology Research Centre, Faculty of Science, Universiti Putra Malaysia, 43400 UPM Serdang, Selangor, Malaysia*
[5] *Sustainable Energy Technologies (SET) Center, College of Engineering, King Saud University, Riyadh 11451, Saudi Arabia*
[6] *Department of Chemistry, University of Sargodha, Sargodha 40100, Pakistan*
[7] *Institute of Advanced Technology, Universiti Putra Malaysia, 43400 UPM Serdang, Selangor, Malaysia*

Correspondence should be addressed to Shaukat Ali Shahid; shaukatuafpy@uaf.edu.pk
and Yun H. Taufiq-Yap; yap@science.upm.edu.my

Received 7 April 2013; Revised 29 June 2013; Accepted 30 June 2013

Academic Editor: Jiaguo Yu

High functional $ZrFe_2O_5$ nanoparticles were synthesized using coprecipitation technique. The chemical composition of nanomaterials was studied by energy-dispersive X-ray (EDX). To observe the morphology, field emission scanning electron microscopy (FE-SEM) was used. X-ray diffraction (XRD) technique was utilized to appraise the structure of the synthesized material. The photocatalytic behavior of $ZrFe_2O_5$ nano-particles was investigated by measuring the degradation rate of toluidine blue O (TBO) dye in aqueous solution in the presence of $ZrFe_2O_5$ nano-particles under visible light irradiation. A steady decrease in absorption peak under visible light irradiation was observed by increasing exposure time. The degradation efficiency was observed as 92% after 140 min of exposure to visible light. Besides, $ZrFe_2O_5$ nanophotocatalyst could be recovered and recycled easily. The rate of TBO and total organic carbon (TOC) removal under visible light irradiation decreased by only 5% and 10%, respectively, after seven cycles of use, demonstrating the high photostability of the synthesized nano-photocatalyst material.

1. Introduction

Over the past few decades, environmental and water decontamination issues have become the foremost area of the scientific research [1–3]. To cope with such issues, there has been great interest among scientists in developing semiconductor photocatalysts with great prospective for environment protection applications such as air purification and water disinfection [1–7].

Among various photo-catalysts, transition metal oxides, such as TiO_2 [6] and $NaNbO_3$ [7], constitute a fascinating and promising class of semiconducting photocatalyst materials that have been widely studied for their photocatalytic activities under UV/Visible light. However, their industrial use in waste water treatment is limited due to their poor visible light absorption capability, reclaiming, and low quantum yield due to fast recombination of charge carriers generated by visible light irradiation [8]. In general, to utilize the visible part of the electromagnetic spectrum ($\lambda > 400$ nm), the bandgap of a photo-catalyst material must be narrow (up to 3.0 eV), and the preferred range of ionic character is between 20 and 30% [9–12].

Searching for new types of potential photo-catalytic materials that can be exploited by solar irradiation particularly under visible light ($\lambda > 400$ nm) along with providing better stability by separating the electron-hole pairs more effectively has become an imperative issue in current photocatalysis and environmental research areas [1–10]. In this regard, better photo-catalytic activity has been observed on a few semiconductor composites combining $ZrFe_2O_5$ with secondary semiconductor, such as TiO_2 under visible light irradiation [13].

Therefore, we were motivated to prepare $ZrFe_2O_5$ with the expectation of improved catalytic performance. Furthermore, to the best knowledge of authors, $ZrFe_2O_5$ has neither been synthesized, nor its photocatalytic behavior has been reported in the literature. Hence, bridging the research gap in photocatalysis using novel $ZrFe_2O_5$ nanomaterial is imperative. Hence, in the present work, we report synthesis of $ZrFe_2O_5$ nanoparticles by coprecipitation technique and the investigation of their photo-catalytic properties under visible light irradiation for the degradation of toluidine blue O dye.

2. Experimental

2.1. Materials. All the chemicals ($ZrOCl_2{\cdot}8H_2O$, $FeCl_3{\cdot}6H_2O$, NH_4OH, and toluidine blue O 85% dye contents) used in the synthesis were purchased from Sigma Chemical Co. (St. Louis, MO, USA) and were used without further purification.

2.2. Synthesis of $ZrFe_2O_5$ Nanoparticles. The $ZrFe_2O_5$ nanoparticles were synthesized by chemical co-precipitation technique [14], in which 50 mL solution A of $ZrOCl_2{\cdot}8H_2O$ was prepared by dissolving "a" grams in deionized water $FeCl_3{\cdot}6H_2O$ and solution B was prepared by dissolving "b" grams in 50 mL as shown in Table 1. Solutions A and B were mixed slowly and stirred for 30 min at 65°C. To precipitate chloride precursors, the pH of the solution was raised to 10 by adding 3.5 M NH_4OH dropwise with continuous stirring; this process took about 120 min. The resulting mixture was left stirred for another 60 min. The precipitate of $ZrFe_2O_5$ was filtered and washed with de-ionized water till chloride became free. The precipitate obtained was dried at 100°C for 90 min in an oven and calcined at 400°C for 4 hours in a muffle furnace.

2.3. Characterization. The structural analysis of $ZrFe_2O_5$ nano-photocatalyst was performed using field emission scanning electron microscope (JEOL JSM 7401 F), energy-dispersive X-ray analysis, and X-ray diffractometer (D8 FOCUS 2220 Bruker AXS) with Cu Kα radiation (λ = 1.5418 A°). Photocatalytic degradation studies were performed by using UV/Vis spectrophotometer (Shimadzu-3600, Japan).

2.4. BET Specific Surface Area Determination. BET specific surface area was determined by N_2 adsorption at (77 K) with a Micromeritics ASAP 2000 system following the overnight treatment to degas the sample in vacuum at 130°C.

2.5. Photocatalytic Activity Test. The reaction mixture was prepared by adding the $ZrFe_2O_5$ nanopowder catalyst (6 mg/L) to TBO dye solution having an initial concentration (C_o) of 0.05 mM. The mixture was then shifted into a glass reactor, where it was stirred for 30 min in dark to attain the adsorption equilibrium [10]. After the adsorption-desorption process, the reaction mixture was irradiated with visible light under constant stirring in oxygen atmosphere. In the photoreaction, the mixture was exposed to visible light ($\lambda \geq$ 510 nm) using a visible lamp (150 W) and a UV cut-off filter. After starting the irradiation process, 3 mL suspension was taken out (with 20 min time intervals) from irradiated mixture and immediately centrifuged at 4000 rpm for 5 min to separate the catalyst nano-particles from the suspension. Absorption of clear solution was taken using UV-Vis spectrophotometer (Shimadzu 3600, Japan) at 30°C and ambient pressure.

Table 1: Amounts of $ZrOCl_2 \cdot 8H_2O$ and $FeCl_3 \cdot 6H_2O$ in solutions A and B.

Sample no.	$ZrOCl_2 \cdot 8H_2O$ "a" g/50 mL in solution A	$FeCl_3 \cdot 6H_2O$ "b" g/50 mL in solution B	$ZrO_2 : Fe_2O_3$ (molar)
S1	1.62	2.72	1 : 1
S2	1.62	2.04	4 : 3
S3	1.62	1.36	2 : 1
S4	1.62	0.68	4 : 1

The percentage of degradation D% was calculated using equation [10]:

$$D\% = \frac{\overset{\circ}{A} - A}{\overset{\circ}{A}} \times 100, \quad (1)$$

where $\overset{\circ}{A}$ and A are the absorbance of the mixture before and after degradation, respectively.

2.6. Stability and Reusability Test. Photo-catalyst activity of same $ZrFe_2O_5$ nanomaterial was tested repeatedly for seven (7) times. After each use, photo-catalyst was separated, washed, dried and 3 mg of fresh photo-catalyst was added at the end of each cycle to compensate for the loss of catalyst during use.

2.7. Total Organic Carbon (TOC) Removal Test. TOC removal was estimated to check mineralization of TBO with $ZrFe_2O_5$ (Figure 6). The values of TOC were determined from illuminated mixture of 0.05 mM dye concentration and catalyst load of 6 mgL^{-1} using TOC analyzer (Thornton 770 Max with 5000TOC sensor).

The degree of TBO mineralization was estimated by determining the decrease in TOC in the reaction solution [10].

3. Results and Discussion

3.1. Characterization of $ZrFe_2O_5$. FE-SEM images of the as-synthesized $ZrFe_2O_5$ nano-particles (ZrO_2 : Fe_2O_3 = 1 : 1) are shown in Figure 1. FE-SEM analysis showed that

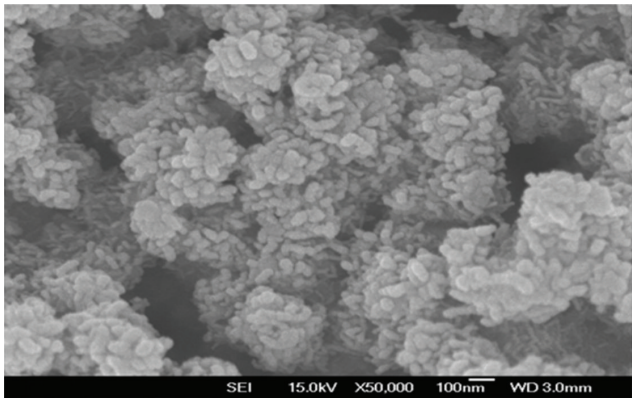

Figure 1: FE-SEM images of $ZrFe_2O_5$ sample S1 after annealing at 400°C for 4 hours.

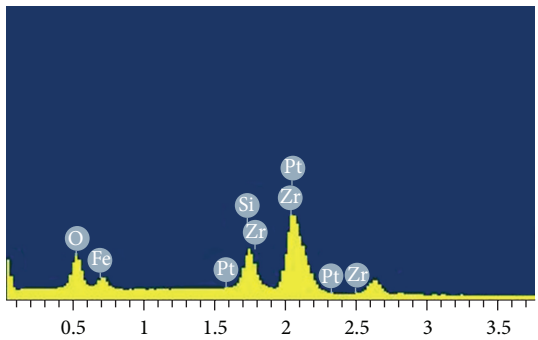

(a)

Element	Weight (%)	Atomic (%)
OK	27.84	61.67
SiK	7.34	9.26
FeK	19.92	12.46
ZrL	39.97	15.53
PtM	4.92	0.89
Totals	100.00	

(b)

Figure 2: (a) EDX elemental analysis of $ZrFe_2O_5$ nanoparticles and (b) chemical composition of $ZrFe_2O_5$ nano-particles determined by EDX.

$ZrFe_2O_5$ nano-particles comprise a mean diameter of 30 nm. The chemical composition of the $ZrFe_2O_5$ nano-particles was appraised by energy dispersive X-ray analysis (EDX) as shown in Figure 2. It is clear from Figure 2(b) that for the 1 : 1 molar ratio, the average composition of Zr/Fe is 68 : 32.

The phase and crystallinity of $ZrFe_2O_5$ nano-particles before and after the calcinations were examined by X-ray diffraction technique on an MX Labo powder diffractometer using Cu Ka radiation (40 kV, 20 mA), at the rate of 2°/min over the range of 20–80°. The XRD patterns showed that $ZrFe_2O_5$ nano-particles were amorphous prior to calcinations (Figure 3(a)). However, after calcinations at 400°C for 4 hours, the nano-particles had transformed into a crystalline $ZrFe_2O_5$ phase (Figure 3(b)).

3.2. Bandgap Energy. Prior to investigating the photocatalytic action, it is imperative to appraise the optical absorption of the $ZrFe_2O_5$ nano-particles for the motive that the UV Vis absorption edge is associated with energy band of the semiconductor catalyst [15]. The optical bandgap (Eg) of $ZrFe_2O_5$ nano-particles estimated from the Tauc plot is 2.4 eV, signifying that the synthesized nanomaterial can absorb visible light.

3.3. UV/Vis Absorption Spectra of TBO Degradation. UV/Vis absorption spectra of TBO degradation with $ZrFe_2O_5$ over a period of 120 min by absorbing visible light are shown in Figure 4.

3.4. Mechanism of Photocatalytic Reactions. The photocatalysis using visible light/$ZrFe_2O_5$ is based on adsorption of photons with energy higher than 2.4 eV ($\lambda \geq 510$ nm), resulting in initiating excitation related to charge separation event. High-energy excited states of electron and hole pairs arise when semiconductors possessing wide band gap are subjected to irradiation higher than their band gap energy. The outcome is the promotion of an electron in the conductive band (e_{CB}^-) and a positive hole formation in the valence band (h_{VB}^+) as shown in (2). The h_{VB}^+ and e_{CB}^- are powerful oxidizing and reducing agents, respectively. The h_{VB}^+ reacts with TBO dye resulting in its oxidation. Consequently, CO_2 and H_2O are produced as end products (7). The h_{VB}^+ can also oxidize organic compounds by reacting with water to generate $^\bullet OH$ (8). Due to electron preferring nature of hydroxyl radical ($^\bullet OH$), it can oxidize almost all electron rich organic dyes, ultimately converting them to CO_2 and water (9). The conductive band e_{CB}^- can react with O_2 forming an anion radical superoxide as shown in (3). Further reactions can lead to the formation of hydrogen peroxide which leads to the formation of $^\bullet OH$. Consider the following:

$$ZrFe_2O_5 + h\upsilon \ (\lambda \geq 510\,\text{nm}) \longrightarrow ZrFe_2O_5 \ (e_{CB}^- + h_{VB}^+) \quad (2)$$

$$(O_2)_{ads} + e_{CB}^- \longrightarrow {}^\bullet O_2^- \quad (3)$$

$$O_2^- + H^+ \longrightarrow HO_2 \quad (4)$$

$$2HO_2 \longrightarrow H_2O_2 + O_2 \quad (5)$$

$$H_2O_2 + h\upsilon \longrightarrow 2\,{}^\bullet OH \quad (6)$$

$$h_{VB}^+ + \text{TBO} \longrightarrow \text{intermediates} \longrightarrow CO_2 + H_2O \quad (7)$$

$$H_2O + h_{VB}^+ \longrightarrow {}^\bullet OH + H^+ \quad (8)$$

$$^\bullet OH + \text{TBO} \longrightarrow \text{intermediates} \longrightarrow CO_2 + H_2O \quad (9)$$

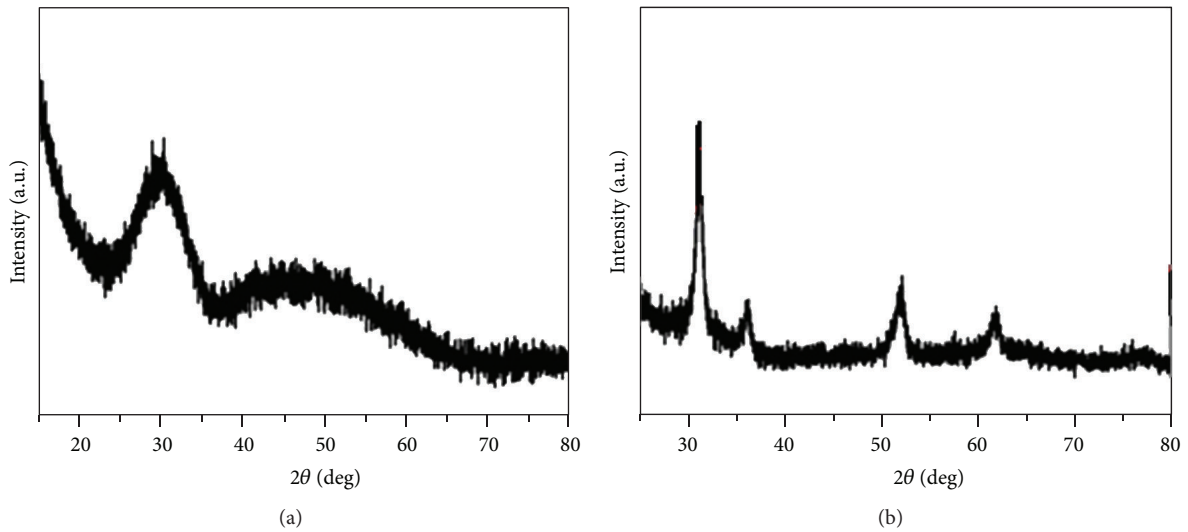

FIGURE 3: XRD pattern of (a) as-grown $ZrFe_2O_5$ nano-particles by co-precipitation at room temperature and (b) $ZrFe_2O_5$ nano-particles after annealing at 400°C for 4 hours.

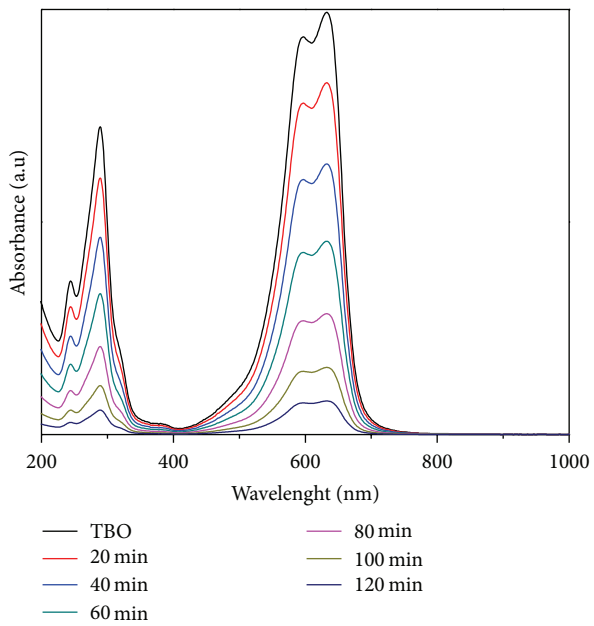

FIGURE 4: UV/Vis Absorption spectra of TBO degradation by S1 ($ZrFe_2O_5$).

During photo-catalytic degradation, the presence of dissolved oxygen restricts the recombination process on $ZrFe_2O_5$ (e_{CB}^-/h_{VB}^+) which results in maintaining the electroneutrality of the $ZrFe_2O_5$ particles. Hence, effective photo-catalytic degradation of TBO dye is achieved by the reduction process of oxygen and the oxidation of TBO simultaneously to avoid the accumulation of electron in the conduction band and thus reducing the rate of recombination of e_{CB}^- and h_{VB}^+.

3.5. Evaluation of Photocatalytic Activity. TBO dye was taken as a test pollutant. The photo-catalytic activity was evaluated by studying the disintegration rates of TBO dye in the presence of samples S1, S2, S3, and S4 under visible light irradiation through a cut-off filter ($\lambda \geq 510$ nm). A 0.05 mM solution of TBO decomposed rapidly under visible light when sample S1 was used, highlighting their photo-catalytic activity. The dye solution was degraded by approximately 92% in 140 min under visible light for sample S1 (Figure 5). However, degradation of dye decreased with the increase in the amount of zirconium in the nano-particles which shows consistency with the optical absorbance results (Figure 4). For comparison we also studied the photo-catalytic behavior of bulk $ZrFe_2O_5$ as shown in Figure 5. The enhancement in the photo-catalytic behavior of $ZrFe_2O_5$ nano-particles can be ascribed to considerably higher specific surface area of nano-particles compared with the bulk $ZrFe_2O_5$ (Table 2).

By contrast, the TBO without $ZrFe_2O_5$ nano-particles as a catalyst under visible light was stable, and only 2% had degraded after 140 min. It is clearly seen from Figure 5 that under visible light, sample S1 of the $ZrFe_2O_5$ nano-particles shows 92% degree of mineralization after 140 min. This is the first report on photo-catalytic degradation of TBO with $ZrFe_2O_5$ nano-particles in a relatively shorter time with a high stability suggesting its reusability. Previously, Shakir et al. [10] observed degree of mineralization as 85% after 3 hours of degradation of TBO with $Cu_{0.33}MoO_3$ nanorods under visible light irradiation. In a new study reported by Ito et al. [16], zirconium ferrite particles were used for elimination of phosphate from water of sewage treatment plants to avert eutrophication of semienclosed bay of Tokyo. They further discovered good adsorbance of phosphate ions onto zirconium ferrite particles. Magnetic separation characteristic indicated that 90% of phosphate in the discharge water of sewage plants could be eliminated in 5 min [16]. Besides, the zirconium ferrite adsorbent could be used repeatedly.

3.6. Stability Evaluation of $ZrFe_2O_5$ Nanophotocatalyst. The photo-catalytic stability and long-term use of these $ZrFe_2O_5$

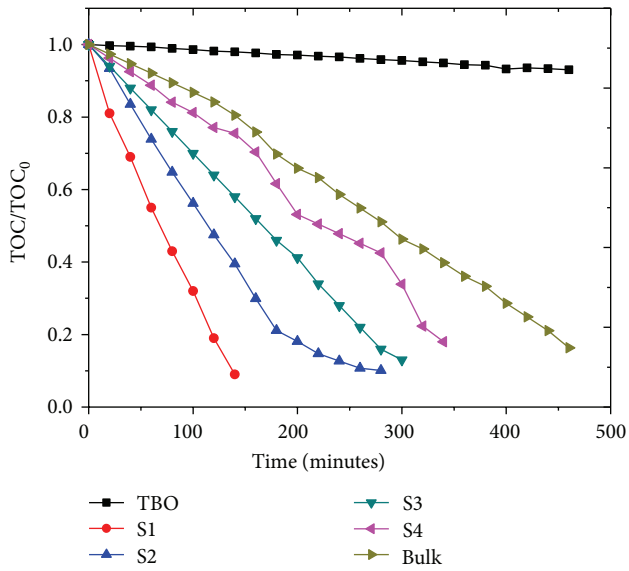

Figure 5: Photo-catalytic degradation profile of the TBO mineralization concentration in the solution (50 mL) with samples S1, S2, S3, and S4 and bulk $ZrFe_2O_5$ versus the exposure time to visible light irradiation.

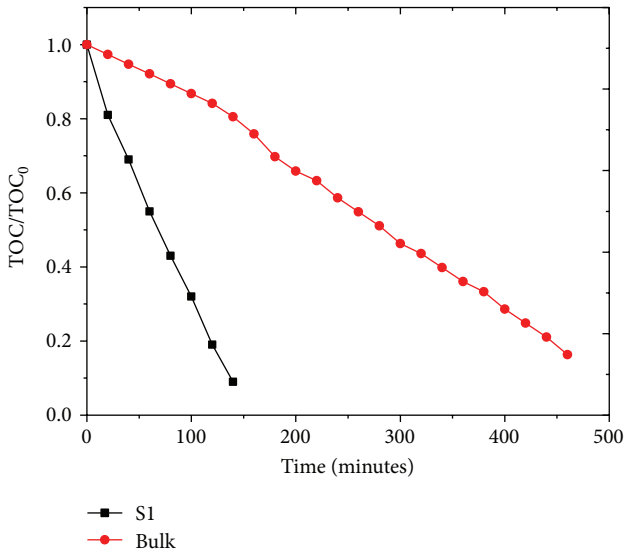

Figure 6: The mineralization rate of contaminant as determined by measuring the disappearance of total organic carbon (TOC) during the photocatalytic degradation of TBO by photocatalysis with $ZrFe_2O_5$ nanoparticles under visible light irradiation.

Table 2: Specific surface area of $ZrFe_2O_5$ nanoparticles of different molar ratios calcined at 400°C and % age degradation of TBO dye.

Sample no.	$ZrO_2 : Fe_2O_3$ (molar)	Crystallite size (nm)	BET specific surface area m^2/g	Degradation of TBO dye
S1	1 : 1	~23	83.14	92%
S2	4 : 3	~26	74.65	81%
S3	2 : 1	~29	63.11	69%
S4	4 : 1	~33	56.92	53%

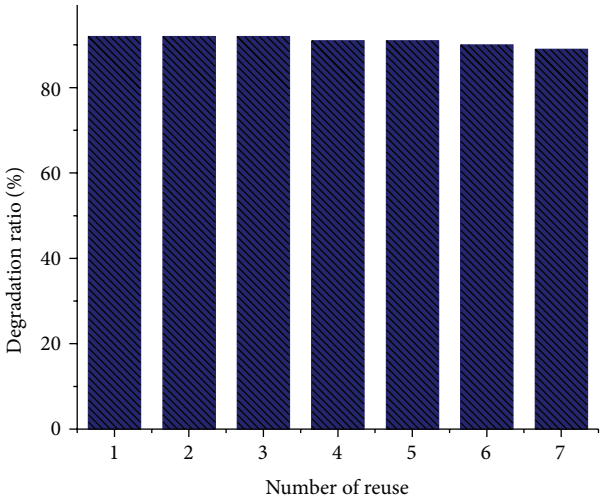

Figure 7: Dependence of the stability of photo-catalytic activity for the photodegradation of TBO under visible light irradiation by reusing the same $ZrFe_2O_5$ nano-particles over seven times under the same conditions.

nano-particles were also evaluated by recycling the photo-catalyst for up to seven reaction cycles and measuring the degradation rates of TBO, as shown in Figure 7. After each photo-catalytic reaction, aqueous solution was centrifuged at 4000 rpm for 5 min to isolate the catalyst from aqueous solution and redispersed it in fresh TBO solution for another cycle. The $ZrFe_2O_5$ nanomaterial showed stable photo-catalytic behavior even after seven (7) cycles of reactions, demonstrating the high photostability of the $ZrFe_2O_5$ nano-particles. The total organic carbon (TOC) was also measured to evaluate the total destruction of TBO (Figure 6). The rate of TBO and TOC removal under visible light irradiation decreased by only 5% and 10%, respectively, after seven cycles, demonstrating the high photostability of the synthesized photo-catalyst against visible light.

One of the factors that improved the photo-catalytic performance of $ZrFe_2O_5$ to a great extent is the size shrinkage of $ZrFe_2O_5$, thereby enlarging its specific surface area, due to which it could adsorb more TBO to photodegrade on its surface. From the electronic structure point of view, the band potentials of $ZrFe_2O_5$ accomplish a straddling gap, which may make possible the transfer of charge carriers and retard the e^-h^+ recombination, ensuring the superior photo-catalytic performance [15, 17–19]. Furthermore, the superior reactivity of the $ZrFe_2O_5$ was observed on samples with appropriate 1 : 1 molar ratios of $ZrO_2 : Fe_2O_3$, suggesting that there is a critical ratio for such a positive synergistic effect. Above this critical ratio, excessive zirconium covers the active sites and hinders the visible light penetration in the sample to excite $ZrFe_2O_5$. This correspondingly deteriorates the photo-catalytic activity, as a consequence of increased recombination of the photogenerated charges on $ZrFe_2O_5$. However, optimum molar ratios of $ZrO_2 : Fe_2O_3$ became the

cause for a quicker separation of electron-hole pair resulting in slower recombination.

4. Conclusions

A new type of photo-catalyst $ZrFe_2O_5$ nano-particles has been synthesized by co-precipitation technique, and its photo-catalytic properties were investigated. The photo-catalytic measurements showed that $ZrFe_2O_5$ nano-particles under visible light could be efficiently used for the photo-catalytic degradation of toluidine blue O dye. Photodegradation efficiency in the absence of $ZrFe_2O_5$ nano-particles showed no significant change in the absorption maximum of toluidine blue O. Although bulk $ZrFe_2O_5$ exhibits the photo-catalytic ability to decompose TBO dye under visible light irradiation, however, degradation with $ZrFe_2O_5$ nano-particles is tremendously more efficient than that of bulk $ZrFe_2O_5$.

Conflict of Interests

Authors have no direct financial relation with the commercial identities mentioned in the paper that might lead to a conflict of interests.

Acknowledgment

This project was supported by Deanship of Scientific Research, College of Science Research Center, King Saud University, Riyadh, Saudi Arabia.

References

[1] P. Qu, J. Zhao, T. Shen, and H. Hidaka, "TiO_2-assisted photodegradation of dyes: a study of two competitive primary processes in the degradation of RB in an aqueous TiO_2 colloidal solution," *Journal of Molecular Catalysis A*, vol. 129, no. 2-3, pp. 257–268, 1998.

[2] P. Peralta-Zamora, S. Gomes de Moraes, R. Pelegrini et al., "Evaluation of ZnO, TiO_2 and supported ZnO on the photoassisted remediation of black liquor, cellulose and textile mill effluents," *Chemosphere*, vol. 36, no. 9, pp. 2119–2133, 1998.

[3] A. L. Linsebigler, G. Lu, and J. T. Yates Jr., "Photocatalysis on TiO_2 surfaces: principles, mechanisms, and selected results," *Chemical Reviews*, vol. 95, no. 3, pp. 735–758, 1995.

[4] W. Cun, Z. Jincai, W. Xinming et al., "Preparation, characterization and photocatalytic activity of nano-sized ZnO/SnO_2 coupled photocatalysts," *Applied Catalysis B*, vol. 39, no. 3, pp. 269–279, 2002.

[5] M. E. Manríquez, T. Lopez, R. Gomez, and J. Navarrete, "Preparation of TiO_2-ZrO_2 mixed oxides with controlled acid-basic properties," *Journal of Molecular Catalysis A*, vol. 220, no. 2, pp. 229–237, 2004.

[6] U. I. Gaya and A. H. Abdullah, "Heterogeneous photocatalytic degradation of organic contaminants over titanium dioxide: a review of fundamentals, progress and problems," *Journal of Photochemistry and Photobiology C*, vol. 9, no. 1, pp. 1–12, 2008.

[7] K. Rajeshwar, M. E. Osugi, W. Chanmanee et al., "Heterogeneous photocatalytic treatment of organic dyes in air and aqueous media," *Journal of Photochemistry and Photobiology C*, vol. 9, no. 4, pp. 171–192, 2008.

[8] X. Li, Y. Hou, Q. Zhao, W. Teng, X. Hu, and G. Chen, "Capability of novel $ZnFe_2O_4$ nanotube arrays for visible-light induced degradation of 4-chlorophenol," *Chemosphere*, vol. 82, no. 4, pp. 581–586, 2011.

[9] G. Mehash, B. Visvanathan, R. P. Visvanath, and T. K. Vardarajan, *Photoelectro—Chemistry and Photobiology in the Environment Energy and Fuel*, Chapter 11, 2007.

[10] M. Shahid, I. Shakir, S.-J. Yang, and D. J. Kang, "Facile synthesis of core-shell SnO_2/V_2O_5 nanowires and their efficient photocatalytic property," *Materials Chemistry and Physics*, vol. 124, no. 1, pp. 619–622, 2010.

[11] K. Naito, T. Tachikawa, M. Fujitsuka, and T. Majima, "Single-molecule observation of photocatalytic reaction in TiO_2 nanotube: importance of molecular transport through porous structures," *Journal of the American Chemical Society*, vol. 131, no. 3, pp. 934–936, 2009.

[12] R. Rahimi, M. Rabbani, and S. S. Moghddam, "Application of N, S-codoped TiO_2 photo-catalyst for degradation of methylene blue," in *Proceedings of the 16th International Conference on Synthetic Organic Chemistry (ECSOC-16 '12)*, November 2012.

[13] W. Fu, Y. Wang, C. He, and J. Zhao, "Photocatalytic degradation of acephate on $ZnFe_2O_4$-TiO_2 photocatalyst under visible-light irradiation," *Journal of Advanced Oxidation Technologies*, vol. 15, no. 1, pp. 177–182, 2012.

[14] I. Ullah, S. Ali, M. A. Hanif, and S. A. Shahid, "Nanoscience for environmental remediation: a review," *International Journal of Chemical and Biochemical Sciences*, vol. 2, no. 1, pp. 60–77, 2012.

[15] Z. Zhang, W. Wang, E. Gao, M. Shang, and J. Xu, "Enhanced photocatalytic activity of Bi_2WO_6 with oxygen vacancies by zirconium doping," *Journal of Hazardous Materials*, vol. 196, pp. 255–262, 2011.

[16] D. Ito, K. Nishimura, and O. Miura, "Removal and recycle of phosphate from treated water of sewage plants with zirconium ferrite adsorbent by high gradient magnetic separation," *Journal of Physics*, vol. 156, Article ID 012033, 2009.

[17] S. Song, F. Hong, Z. He, H. Wang, X. Xu, and J. Chen, "Influence of zirconium doping on the activities of zirconium and iodine co-doped titanium dioxide in the decolorization of methyl orange under visible light irradiation," *Applied Surface Science*, vol. 257, no. 23, pp. 10101–10108, 2011.

[18] C. McManamon, J. D. Holmes, and M. A. Morris, "Improved photocatalytic degradation rates of phenol achieved using novel porous ZrO_2-doped TiO_2 nanoparticulate powders," *Journal of Hazardous Materials*, vol. 193, pp. 120–127, 2011.

[19] A. A. Ashkarran, S. A. A. Afshar, S. M. Aghigh, and M. kavianipour, "Photocatalytic activity of ZrO_2 nanoparticles prepared by electrical arc discharge method in water," *Polyhedron*, vol. 29, no. 4, pp. 1370–1374, 2010.